

Micromagnetic Modeling of Spin-valve MR Head with Synthetic Antiferromagnet (SyAF)

Y. W. Tahk^{1,*}, K. J. Lee² and T. D. Lee¹

¹Dep. of Materials Sci. and Eng., Korea Advanced Institute of Science and Technology, Yusong, Taejeon 305-701, Korea

²Storage Lab. Samsung Advanced Institute of Technology, P.O. Box 111, Suwon, Korea

(Received 8 May 2002)

MR transfer behaviors of the permanent magnet biased spin valve MR sensors with SyAF (synthetic antiferromagnet) layers were studied by micromagnetics modeling. For narrow track MR heads, various height to width ratios were considered together with strength of permanent magnets which stabilizes the free layer. As the MR sensor width is reduced to 0.12 μm , sensor height less than 0.09 μm is needed to show good linearity and the Mr-t of permanent magnets smaller than 0.2 memu/cm^2 is sufficient for the domain stabilization. The conditions for single domain behavior of the free layer were also investigated through optimizing the biasing strength of permanent magnet, the shield gap and the aspect ratio of MR sensor.

Key words : synthetic antiferromagnet, micromagnetics modeling, spin valve, MR head

1. Introduction

In a spin-valve type MR sensor used as a read head for high density magnetic recording, the magnetization behaviors of a pinned layer and a free layer should be stably controlled so that sensors have a wide dynamic range and a good linear response [1-3]. The sensors with a synthetic antiferromagnet (Co/Ru/Co) [4-6] have improved thermal and magnetic stabilities compared to the conventional spin-valve sensors with a single pinned layer. In view of linear MR response, to find the conditions for single domain behavior of the free layer would be helpful. In the present study, micromagnetic modeling for the MR transfer behaviors of the permanent magnet biased GMR heads which have a AF/Co_(pinned)/Ru/Co_(reference)/Cu/NiFe_(free)-type SyAF(synthetic antiferromagnet) spin-valve structure was performed to study the correlation between head geometry parameters and read back properties.

2. Model and Geometry

We have developed a 3-dimensional micromagnetic model to study permanent magnet biased MR heads with a SyAF (synthetic antiferromagnet). Fig. 1 shows a schematic

drawing of the modeled head structure. In the model, the free layer and two Co layers are discretized into 2-dimensional arrays of tetragonal elements. Co_(pinned) layer is additionally biased by an exchange field of about 500 Oe from the antiferromagnetic layer. The classic micromagnetic theory is used to calculate the free energy in the system, including the antiferromagnetic coupling energy ($\geq 0.25 \times 10^{-6}$ erg/cm) between two Co SyAF layers separated by a thin Ru layer. The imaging effect of the soft magnetic shields is approximated by the imaging of two infinite surfaces with infinite permeability. The saturation magnetization, crystalline anisotropic field and thickness

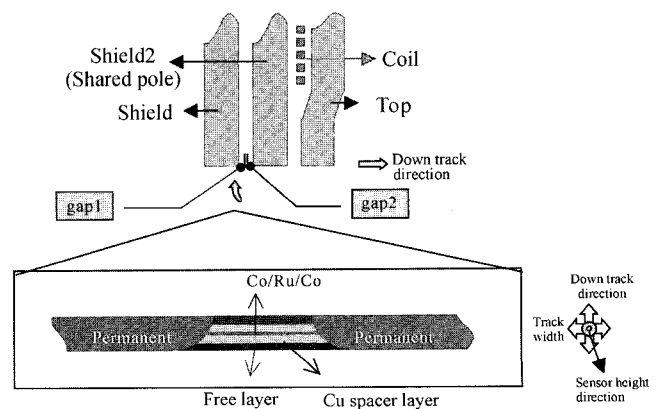


Fig. 1. Schematic of a ring type head with SyAF SV sensor.

*Corresponding author: Tel: +82-42-869-3376, e-mail: narzis@kaist.ac.kr

Table 1. Material parameters

	Free layer	Permanent magnet	Co layer (reference)	Co layer (pinned)
$M_s(\text{emu/cc})$	800	300~625	1422	1422
$H_K(\text{Oe})$	3.5	>5000 Oe	20	20
Easy axis	Uniaxial (sensor width)	3D random	Uniaxial (sensor height)	Uniaxial (sensor height)
Thickness (Å)	25~45	90~120	15~20	20~25

of each magnetic layer are shown in Table 1. Ru layer and Cu layer have a thickness of 7 Å and 20 Å, respectively. The total shunt current through the sensor layers varies in the range of 1~4 mA while the maximum current density is less than $6 \times 10^7 \text{ A/cm}^2$. Shunt bias field is obtained using Biot-Savart's law.

Within each element, the magnetization M varies in time according to the Landau-Lifshitz-Gilbert equation:

$$\vec{M} = -\gamma \vec{M} \times \vec{H}_{eff} - \alpha \gamma \frac{\vec{M}}{M_s} \times (\vec{M} \times \vec{H}_{eff}) \quad (1)$$

The gyromagnetic ratio γ equals $1.76 \times 10^7 \text{ Oe}^{-1} \text{ s}^{-1}$ and the phenomenological damping parameter α of 0.1 is used. MR response is represented by $\langle -\cos(\Delta\theta) \rangle$ where $\Delta\theta$ is the difference in the magnetization directions of the freelayer and the $\text{Co}_{(\text{reference})}$ layer, while the output voltage of MR response is as follows,

$$V = J \cdot W \cdot \Delta\rho \cdot \frac{1 - \cos(\Delta\theta)}{2} \quad (2)$$

where J is sensing current density and W is read track width.

3. Results and Discussion

3.1. Effect of Sensor Height

Fig. 2 shows the calculated MR response transfer curve vs. the signal field at various sensor heights with a sensor width of $W=0.12 \mu\text{m}$. Decreasing the sensor height, h from $0.24 \mu\text{m}$ to $0.06 \mu\text{m}$, the linear dynamic range was improved. The center position of transfer curves at 0 Oe signal field can be controlled by changing the shunt current or the thickness of the two Co layers. As shown in Fig. 2(a), the case of $h=0.24 \mu\text{m}$ ($h/W=2.0$) has obvious hysteresis, which is mainly due to the increased shape anisotropy. Another reason is the excitation field from the written bits decays so fast with a rate exponentially proportional to the distance from ABS that the upper part of the freelayer is overall insensitive to the excitation field and MR response is retarded. These MR response behaviors can be understood through the magnetization

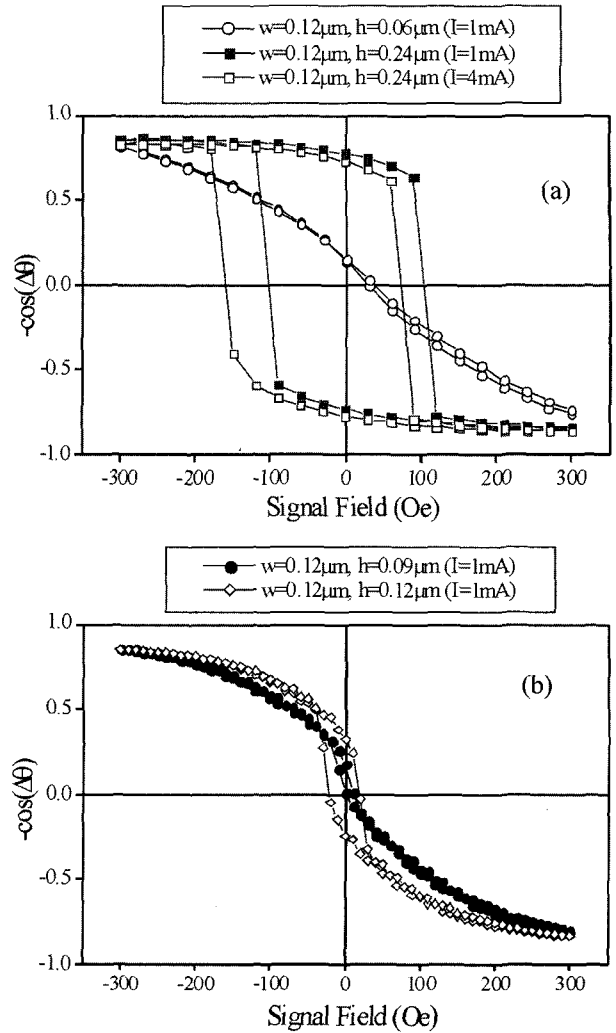


Fig. 2. MR transfer curves of SyAF SV sensor with Free (45 Å)/Cu(20 Å)/SyAF(20 Å/7 Å/20 Å)/IrMn(188 Å), width = $0.12 \mu\text{m}$, $g_1=550 \text{ Å}$, $g_2=350 \text{ Å}$, $M_r(\text{PM})=0.197 \text{ memu/cm}^2$ for various values of the MR height, (a) $0.06 \mu\text{m}$, $0.24 \mu\text{m}$ and (b) $0.09 \mu\text{m}$, $0.12 \mu\text{m}$.

analyses.

Fig. 3 shows the magnetization configuration of the free layer with sensor height of (a) $0.06 \mu\text{m}$ and (b) $0.12 \mu\text{m}$ at the various excitation fields. In the case of Fig. 3(a) with $h/W=0.5$, the remanent magnetization is aligned to the width direction which is parallel to ABS, and there is little hysteresis and this is coincident with the calculation of single domain (SD) model (Fig. 4(a)). In the other hand, the case of Fig. 3(b) shows different remanent magnetizations between $+0 \text{ Oe}$ state and -0 Oe state, where $+0 \text{ Oe}$ state is obtained from reducing signal field from $+300 \text{ Oe}$ to $+0 \text{ Oe}$. This trend is intensified increasing h/W ratio. It can be also deduced from comparison of the MR transfer curves of non-single domain model and single domain model in Fig. 4(b). The hysteresis calcu-

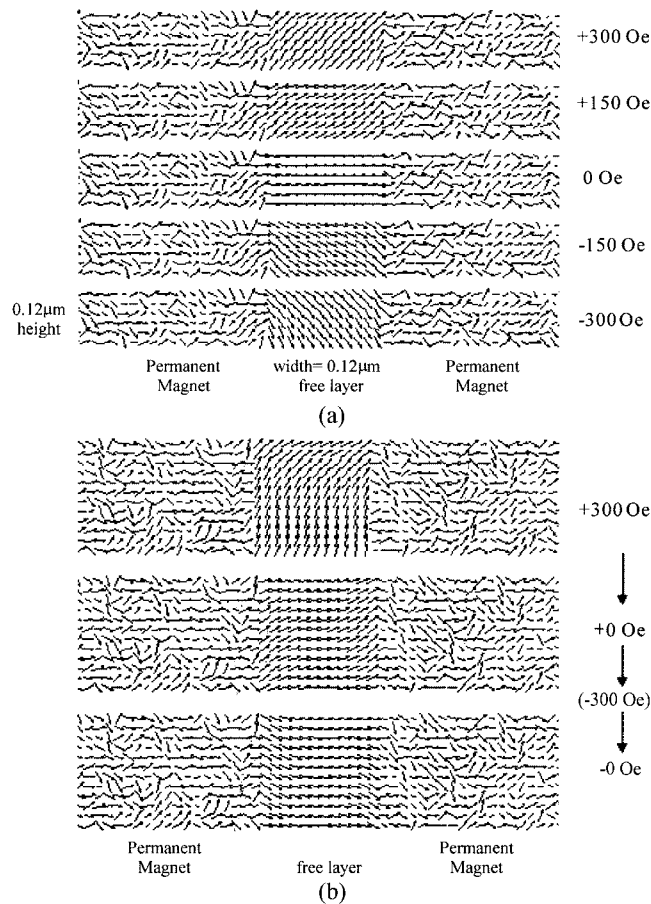


Fig. 3. Magnetization configurations of the free layer at the various excitation fields for (a) height=0.06 μm, (b) 0.12 μm.

lations of higher h/W ratio cases dont agree with those of single domain model.

3.2. Effect of Permanent magnet

Fig. 5 shows the calculated transfer curves with two different sensor height for various area moment density values of the abutting permanent magnet (PM). A large Mrt value yields both lower sensitivity and smaller dynamic range. However, if the Mrt value is too small, the magnetization at the side edges of the free layer will rotate to be partially parallel to the side edges in order to minimize the magnetic surface charge at the interface between free layer and permanent magnet. Signal field will yield irreversible switching of the edge domains, spreading out the hysteresis of transfer curve as shown in Fig. 5(a) for Mrt(PM)=0.197 and 0.075 memu/cm². This weak PM strength can not prevent the multidomain formation in the freelayer. The optimal value of the permanent magnet strength for each case of sensor height =0.09 μm and 0.06 μm is about 0.3 and 0.2 memu/cm², respectively.

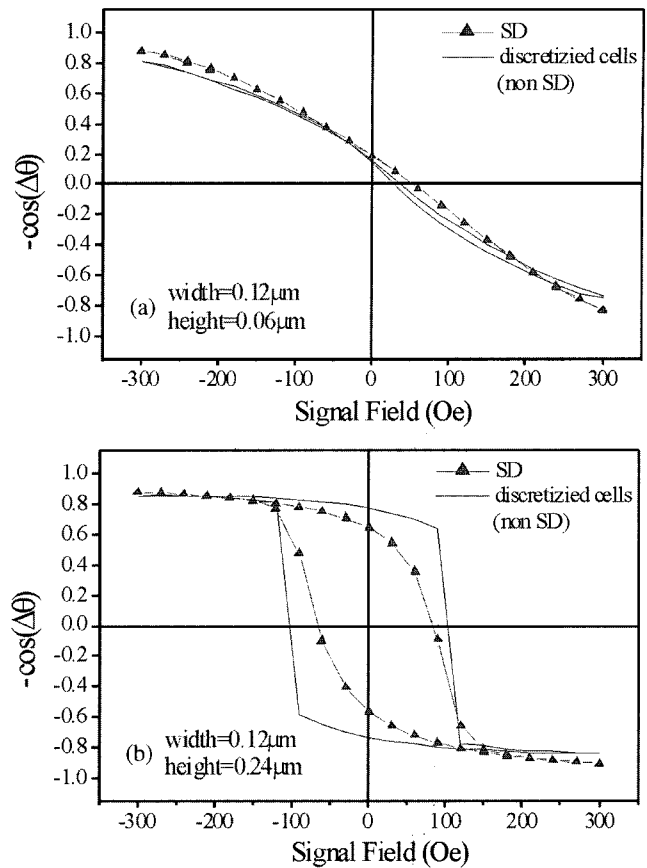


Fig. 4. MR transfer curve comparison of non-single domain model and single domain model for a SyAF biased SV sensor with Free(45 Å)/Cu(20 Å)/SyAF(20 Å/7 Å/20 Å)/IrMn(188 Å), width=0.12 μm, g1=550 Å, g2=350 Å, Mrt(PM)=0.197 memu/cm² and (a) height=0.06 μm and (b) height=0.24 μm.

3.3. Effect of Magnetic layer Thickness

In this section, the effects of changes in the thickness of the freelayer and Co layers were investigated. Fig. 6 shows MR transfer curves of two MR sensors with different freelayer thickness of 45 Å and 25 Å. The steeper slope and more sensitive response to the signal field were shown in the transfer curve for the case of 25 Å. This phenomenon is easily understood from the fact that switching field of thinner free layer is much smaller than that of thicker one.

4. Conclusion

For small sized MR heads, various height to width (H/W) ratios were considered together with the bias field strength of permanent magnets which stabilizes the free layer. As the MR sensor width is reduced to 0.12 μm, sensor height less than 0.09 μm is needed to show good linearity and the Mrt of permanent magnets smaller than

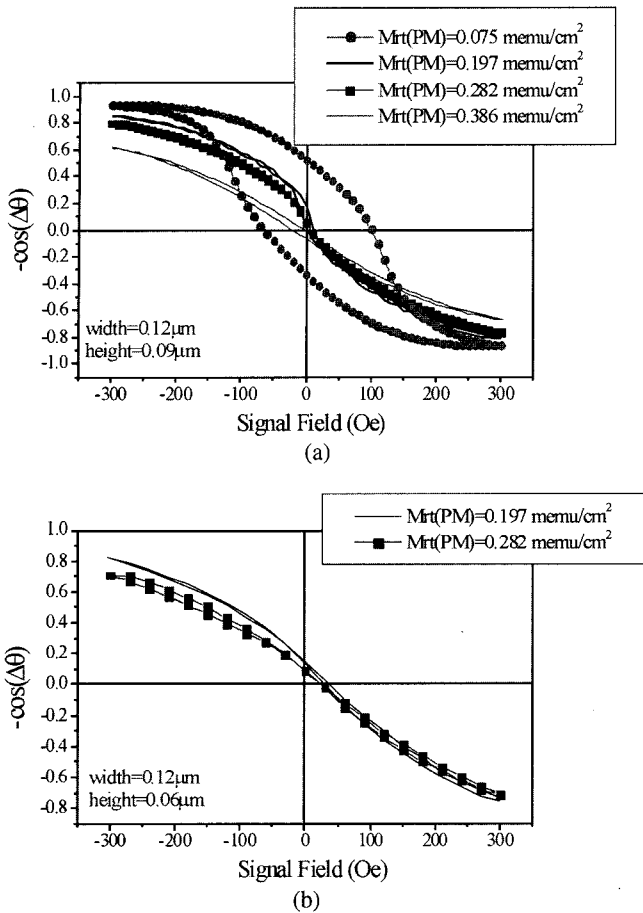


Fig. 5. MR transfer curves of Free(45 Å)/Cu(20 Å)/SyAF(20 Å/7 Å/20 Å)/IrMn(188 Å), $g_1=550$ Å, $g_2=350$ Å and the different $M_r t$ (PM). (a) width=0.12 μm , height=0.09 μm (b) width=0.12 μm , height=0.06 μm .

0.2 memu/cm^2 is sufficient for the domain stabilization.

It was found that there is a boundary where the free layer behaviors as a nearly single domained particle depending on the strength of permanent magnet, the shield gap and the aspect ratio of MR sensor. When the

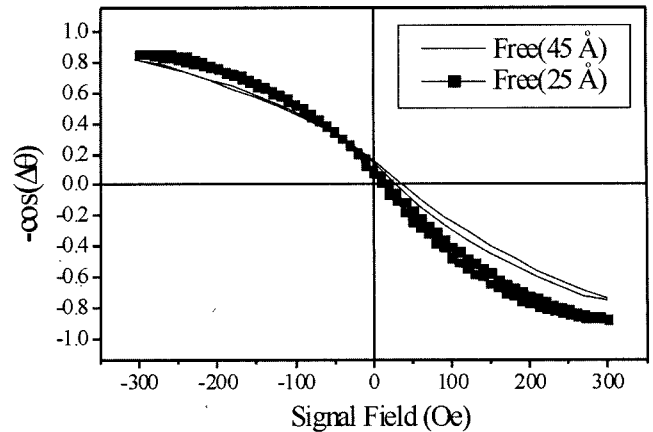


Fig. 6. MR transfer curve of Free/Cu(20v)/SyAF(20 Å/7 Å/20 Å)/IrMn with width=0.12 μm , height=0.06 μm , $g_1=550$ Å, $g_2=350$ Å, $M_r t$ (PM)=0.197 memu/cm^2 for two cases of free layer thickness, 45 Å and 25 Å.

MR sensor width is 0.12 μm and the $M_r t$ of the permanent magnets is 0.384 memu/cm^2 , the results of the two models coincide for sensor height less than 0.09 μm . However, when the $M_r t$ of the permanent magnets decreases to 0.2 memu/cm^2 the sensor height also should be reduced to 0.06 μm or less to show a single domain behavior of the free layer.

References

- [1] D. E. Heim et al., IEEE Trans. Magn. **30**, 316 (1994).
- [2] R. E. Fontana et al., IEEE Trans. Magn. **35**, 806 (1999).
- [3] K. R. Coffey et al., U.S. Patent No.5583725 (10 Dec. 1996)
- [4] J. L. Leal and M. H. Kryder, J. Appl. Phys. **83**(7), 3720 (1998).
- [5] S. S. P. Parkin et al., Phys. Rev. Lett. **64**(19), 2304 (1990).
- [6] J. G. Zhu, IEEE Trans. Magn. **35**, 655 (1999).